

Effect of Lignin-containing Highly Fibrillated Cellulose on the Adsorption Behavior of an Organic Dye

Zhongyu Yan,^a Caifu Yi,^b Tao Liu,^c Jiawan Yang,^c Haizhu Ma,^e Lizheng Sha,^{a,*} Daliang Guo,^a Huifang Zhao,^a Xiaoqin Zhang,^d and Wenjun Wang^d

The morphological properties and particle size characteristics of micro- and nanofibrillated cellulose (NFC) and lignin-containing NFC (LNFC) produced by a microfluidizer processor were investigated. The effects mechanism of lignin-containing on the adsorption of NFC and the stable properties of organic dyes suspension were also studied. The results showed that the preparation process and final performance of NFC were affected by the key factors including lignin, homogenization pressure, and number of homogenization cycles. The increase in the homogeneity of the fibrillated cellulose was minor for the NFC samples, while LNFC samples showed a larger increase in the homogeneity of the particle size distribution. The influence of lignin was reflected both in improved fibrillation efficiency and in the final organic dye dispersion properties achieved by LNFC addition, primarily observed as decreased particle sizes and fibril dimensions. This study indicated that pollution-free dispersion of organic dyes can be realized through the application of lignin-containing NFC.

Keywords: Cellulose microfibril; Lignin-containing microfibrillated cellulose; Organic dyes; Suspension; Morphological

Contact information: a: School of Environmental and Natural Resources, Zhejiang University of Science and Technology, Hangzhou, China; b: Zhejiang Hengda New Material CO., LTD, Quzhou, Zhejiang Province, China; c: Zhejiang Shanying Paper CO., LTD, Haiyan, Zhejiang Province, China; d: Hangzhou Haile Electrical CO., LTD, Hangzhou, Zhejiang Province, China; e: Engineering Research Center for Eco-Dyeing & Finishing of Textiles, Ministry of Education, Zhejiang Sci-Tech University, Hangzhou, China; * Corresponding author: slz9966@163.com

INTRODUCTION

Nanofibrillated cellulose (NFC) is a promising eco-friendly biomaterial that has some advantages such as being low-density, renewable, biodegradable, and non-toxic, as well as having other good physical properties (Vanhatalo *et al.* 2016). Therefore, NFC is expected to play an important role in many industries including thermoplastic matrix materials, drug delivery, packaging materials, *etc.* (Lissi and Abuin 2000; Rivers *et al.* 2019). In the present work, the term NFC is used in a broad sense to include cellulosic material that has been subjected to high levels of hydrodynamic shearing. The term “microfibrillated cellulose” is often used when the extent of such shearing is not sufficient to convert most of the material so that the fibril widths are less than 100 nm.

Many methods for producing NFC have been published, and these methods are generally using a multistep sequence comprised of mechanical, chemical, or enzymatic processes (Rivers *et al.* 2019). According to the literature (Velasquez-Cock *et al.* 2016; Kawee *et al.* 2018), the characteristics of the NFC are obviously affected by the pretreatment methods, microfabrication process, and the raw material. For example, Gourlay *et al.* (2018) assessed that the influence of the endoglucanases pretreatment on the

rheological properties of NFC suspensions, and they found that the viscosity properties of NFC were significantly increased by using very low enzyme loadings (0.5 mg/g). Ren *et al.* (2014) produced NFC by using a combination of acid hydrolysis and high-pressure homogenization processes, and they observed that the high-pressure homogenization treatment helped separate the fiber bundles, and the number of homogenization treatments reduced the dimension of the nanocrystals produced. Vanhatalo *et al.* (2016) used a microfluidizer to produce NFC from four different raw materials, and the results indicated that the structural, chemical, and physical characteristics of the raw materials were affected by the process performance and the fibril cellulose properties. Moreover, they reported that the crystallinity of cellulosic structures was reduced with the number of homogenization treatments increasing. Therefore, it can be seen that different pretreatment methods can produce NFC with different properties.

In recent years, several studies showed that a small percent of lignin can affect the properties of cellulose fiber and related nanocellulose. Professor Zhu's group made huge contributions on lignin-containing cellulose nanocrystals (LCNC) and nanofibrils (LCNF) production, especially on the effect of lignin on the properties of LCNF (Bian *et al.* 2017a, b, 2019, 2020; Cai *et al.* 2020). Specifically, Bian *et al.* (2017a) integrated production of LCNC and LCNF using an easily recyclable di-carboxylic acid. They found that the higher lignin content sample resulted in LCNF with a smaller height (diameter) of 7 nm but a longer length of over 1 μm . Meanwhile, Bian *et al.* (2017b; 2020) believed that the physical and chemical properties of the LCNF can be tailored by adjusting the severity of p-toluenesulfonic acid fractionation as well as the intensity of mechanical fibrillation. Bian *et al.* (2019) proposed that mixed enzymatic pretreatment was more suitable for LCNF production, resulting in a smaller average-number height of 15 nm. Cai *et al.* (2020) revealed that lignin esterification (carboxylation) enhanced the lubrication effect of lignin in mechanical nanofibrillation for producing cellulose nanofibrils. Aditiawati *et al.* (2018) investigated that the effect of the delignification process of oil palm empty fruit bunch by inoculum of *Marasmius* sp. and cellulase enzyme on the structural properties of cellulose nanofibrils (CNF); they concluded that the enzyme treatment was conducive to producing CNF with the best size. Lê *et al.* (2018) produced lignin-containing CNF (LCNF) suspensions from the unbleached pulps by pure mechanical treatment, and the results indicated that the presence of lignin had a large impact on the dewatering of cellulose nanofibrils. Herzele *et al.* (2016) studied the properties of microfibrillated lignocellulose (LNFC) obtained from a high-pressure homogenizer in an ethanol/water mixture, and they noticed that LNFC achieved better dispersion of fibrils compared to the default NFC. Meanwhile, Wang *et al.* (2018) used unbleached pulp with high residual lignin content as a raw material for produce LNFC, and they revealed that there was better dispersion of LNFC in organic solvent compared to NFC. Although there has been some research about the effect of lignin on the properties of NFC or CNF, the effect of lignin-content on the dispersion mechanism of NFC, peculiarly the application of dispersed organic dyes for LNFC has not been mentioned.

For this purpose, NFC and lignin-containing NFC (LNFC) were firstly prepared by using a microfluidic high-pressure homogenizer at different homogenization pressures (2500 to 25,000 psi, which is equivalent to 17.2 to 172 MPa) and homogenization cycles (2 and 20 cycles). Secondly, the surface morphology, the particle size distribution, and the crystallinity of NFC and LNFC were characterized by a video microscope, scanning electron microscopy (SEM), Malvern laser particle size analyzer, and X-ray diffraction (XRD), respectively, to confirm the effect of lignin-containing on NFC properties. Finally, the adsorption stability of NFC and LNFC, and the organic dye dispersion stability of NFC

and LNFC were evaluated using a Turbiscan lab stability analyzer. The research results of this study can contribute to the development of a green renewable organic dye dispersant system based on lignin-containing cellulose microfibrils.

EXPERIMENTAL

Materials Pretreatment

NFC and LNFC were prepared from unbleached kraft softwood pulp (Zhejiang Shanying Paper Co., Ltd., Jiaying, China). The major chemical composition of the pulp was analyzed following the same methods as in the previous research (Ehman *et al.* 2020), and the results were 78.2% cellulose, 11.9% hemicellulose, and 9.9% total lignin. To remove the residual lignin, the unbleached pulp fibers were bleached with a 1:1 solution of H₂O₂ (24% v/v) and NaOH (4% w/w) at 55 °C under constant stirring for 3 h. After treatment, the suspension was filtered and washed with distilled water to reach neutral pH. The chemical composition of the bleached pulp fibers was 89.9% cellulose, 8.4% hemicellulose, and 1.7% lignin. The crystallinity values of unbleached and bleached kraft softwood pulp were 48.5% and 53.5%, respectively.

Secondly, the bleached and unbleached pulp (50 g) were added to 200 ppm neutral cellulase, respectively, then stirred for 10 min, and the enzymatic pretreatment (Hangzhou Xili Kang Chemical Co., Ltd., Shandong, China) time was 30 min. Finally, the enzymatically pretreated pulp was refined using a PFI refiner (TB7-FFV, Xianyang Tongda Light Industry Equipment Co., Ltd., Shandong, China) for 47,000 revolutions for 30 min.

High-Pressure Homogenization

1% concentration of NFC and LNFC samples were prepared by using a high-pressure microfluidizer (LM40, Microfluidics International Corporation, USA) at pressure levels ranging from 2500 to 25000 psi (17.2 to 172 MPa) with 2 to 20 cycles, respectively. The experimental conditions are presented in Table 1.

Table 1. Summary of the High-Pressure Homogeneous Experimental Conditions

Sample name	Cycles	Pressure (psi)	Mark
Cellulose Microfibrils (NFC)	Two	2500	NFC1
		25000	NFC2
	Twenty	2500	NFC3
		25000	NFC4
Lignin-containing Cellulose Microfibrils (LNFC)	Two	2500	LNFC1
		25000	LNFC2
	Twenty	2500	LNFC3
		25000	LNFC4

Preparation of Organic Orange Disperse Dyes

Organic dye was used as raw material to prepare the disperse dyes in this study. The chemical formula of the organic orange dye is 2-[N-(2-cyanoethyl)-4-[(2,6-dichloro-4-nitrophenyl) azo] anilino] ethyl acetate (C₁₉H₁₇C₁₂N₅O₄), and the molecular weight is 450.27 g/mol. Twenty g of organic dye was slowly dropped into 30 g of an aqueous solution consisting of deionized water at room temperature, stirring until a homogeneous suspension was obtained. Five g of the organic dye suspension was dispersed in 0.1%

concentration of LNFC and NFC aqueous solution for 30 min at 35 °C by ultrasonic waves (input power 1100 W) to obtain the LNFC and NFC organic orange disperse dyes.

Morphology Analysis

The morphologies of the NFC and LNFC samples were directly characterized by using a Leica DVM6 video microscope (Leica, Germany) in the liquid phase to infer the influence of lignin on the high-pressure homogenization process. A drop of 0.01 wt% fiber suspension was placed on a glass slide and overlaid with a coverslip, then photographed at different magnification. The surface morphologies of the NFC and LNFC obtained from the 25000 psi pressure homogenization process were also determined by using a vltra55 scanning electron microscope (Carl Zeiss SMT co., LTD., Oberkochen, Germany).

Particle Size Measurement

The particle size distribution of the samples was measured with a Malvern MS3000 laser particle size analyzer (Malvern, UK). About 5 mL of the sample was mixed with 250 mL of water using a dispersion unit at an 800 rpm stirring rate. Meanwhile, the suspension remained in an ultrasonic state with an amplitude of 40%. The particle size testing conditions were set as follows: using the standard operating procedure in water dispersing agent at room temperature of 25 °C. The particle refractive index is 1.59, the particle absorption rate is 0.01, and the dispersing agent refractive index is 1.33. The background signal measurement was done with distilled water each time prior to sample measurement. The same sample was measured with multiple repetitions, and the data results were reported as an average of multiple repeats.

Crystallinity Analysis

The crystalline structure of the cellulose was determined using a Thermo Electron XRD-ARL X'TRA-055 diffractometer (Waltham, MA, USA) using Cu-Ka1 as a radiation source at 40 kV and 40 mA. The recorded patterns ranged from 5° to 50° at 0.2 s/step. NFC and LNFC samples were dried by freeze-drying method to prepare powder, and then the powder samples were tested. An estimation for the cellulose crystallinity was made by calculating the crystallinity index (I_{cr}) following the Segal method according to the previous research (Baheti and Militky 2013; Taheri and Samyn 2016),

$$I_{cr} = \frac{I_{002} - I_{am}}{I_{002}} \times 100\% \quad (1)$$

where I_{002} is the intensity of the diffraction from the 002 plane at $2\theta=22.6^\circ$, and I_{am} is the intensity of the background scatter measured at $2\theta=18.7^\circ$. It is known that the I_{002} peak corresponds to the crystalline fraction and the I_{am} peak corresponds to the amorphous fraction.

Adsorption Stability Analysis

The measurements were done by using an expert model Turbiscan Lab analyzer (Formulation Inc., Toulouse, France) with Turbisoft software. The instrument operation involved measuring transmitted and backscattered light intensity profiles of the samples. Firstly, the prepared suspension sample of about 20 mL were slowly add into the transparent glass sample bottle at 30 °C. The next step was to gently and vertically lift the prepared sample pool to be tested. At the selected height, the light intensity changes of each scanning measurement were compared to the previous scanning measurement, and the results were accumulated to the total height of the sample. The testing time was 4 h and

the test frequency was each 30 min. Finally, in the multiple light scattering test, the dynamic stability index (TSI) was used to determine the dispersion stability of suspension. Among them, TSI is an evaluation of the stability of the whole dispersion system. The larger TSI is, the worse the stability of the whole dispersion system is.

RESULTS AND DISCUSSION

Morphological Characteristics

The morphology images of NFC and LNFC at pressure (2500 and 25000 psi; 17.2 and 172 MPa) with two cycles were directly characterized by using a Leica DVM6 video microscope, and the results are shown in Fig. 1. These images show a blue background, which indicates that the selected sample table is a black crystal panel. Such an arrangement can increase the light reflected to the sample surface. When the magnification is large, the background will show blue.

As shown in Figs. 1a and 1b, the morphology of NFC1 and LNFC1 could be described as a complete fiber morphology at the low pressure (2500 psi) homogenization process. As the homogenizer pressure rose to 25000 psi, LNFC2 exhibited greater morphological deconstruction, as noted by the increased fiber external surface area and the related increase in microfibril content.

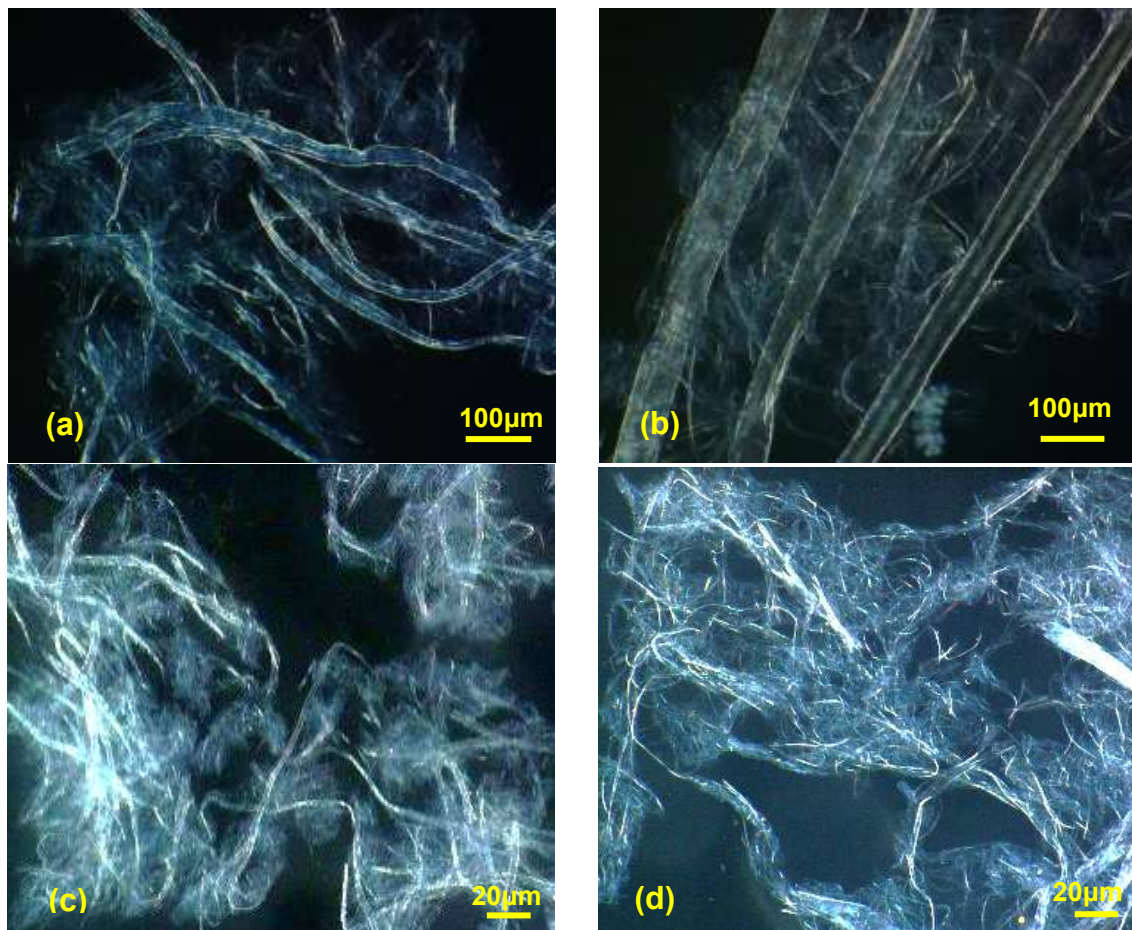


Fig. 1. The morphology of cellulose microfibrils obtained from two cycles of the high-pressure homogeneous process, (a): NFC1, (b): LNFC1, (c): NFC2, and (d): LNFC2

Compared with NFC2, a more disordered network structure was created due to the presence of residual lignin (Chinga-Carrasco *et al.* 2012) (Fig. 1d), while NFC2 showed a state of softening, bending, splitting filaments, and agglomeration (Fig. 1c). The results of the morphological observations indicated that lignin affects the homogenization process of cellulose. Specifically, the lignin-containing samples led to a higher degree of cellulose microfibrillation at high homogenization cycles. A similar result was obtained from the previous research for the preparation of NFC by unbleached pulp with high residual lignin content (Santucci *et al.* 2016). The reason for this phenomenon may be that the presence of lignin prevents the absorption and swelling of the cellulose fiber, which then resists the compression and delamination of cellulose fibers (Wang *et al.* 2012). With greater duration of homogenization, as the lignin-containing fibers are subjected to intense collision, shearing, and cavitation, the fibers are more likely to break up into uniform microfibrillated cellulose during the high-pressure homogenization process.

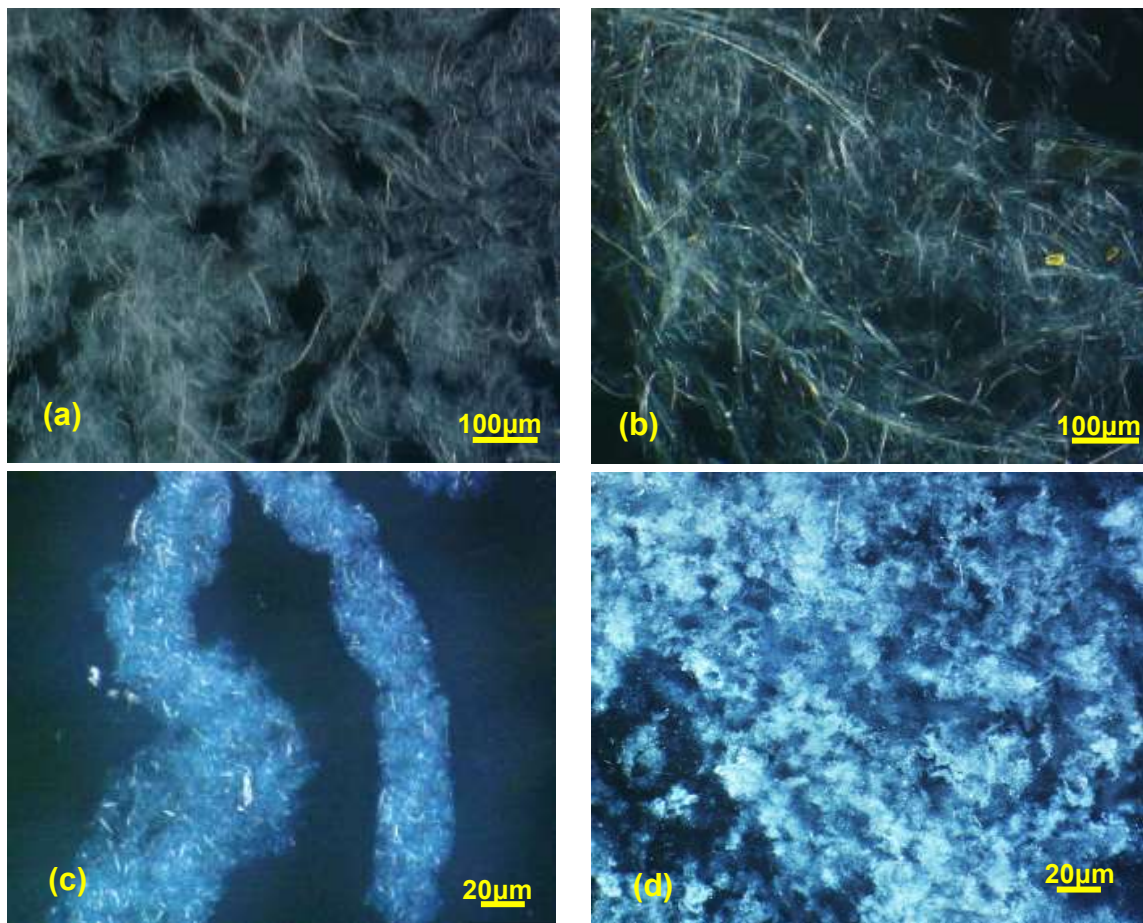


Fig. 2. The morphology of cellulose microfibrils obtained from twenty cycles of the high-pressure homogeneous process, (a): NFC3, (b): LNFC3, (c): NFC4 and (d): LNFC4

Figures 2a and 2b show the morphology of NFC3 and LNFC3 obtained from twenty cycles of the homogeneous process. As shown in Figs. 2a and 2b, the fibers of NFC3 had obviously been cut off, with the forming of flocculated short fibers, while the fibers of LNFC3 appeared as polydisperse and entangled needle fibers. As the pressure rose to 25000 psi, NFC4 and LNFC4 exhibited obvious agglomeration, but greater extents of agglomeration were observed in LCFM4 than in NFC4. Additionally, cell wall residues

and some fibrillated fragments were observed in LCFM4. Meanwhile, in NFC4, smaller and more isolated fibers can be seen. However, the surface morphology of NFC4 and LNFC4 could not be analyzed by the Leica DVM6 video microscope. This indicated that the NFC4 and LNFC4 samples were completely microfibrillated or nanofibrillated, so that the surface morphology of NFC4 and LNFC4 were also analyzed by SEM (Fig. 3).

As shown in Fig. 3, the morphology of LNFC4 exhibited better uniformity than that for NFC4, and this difference could also be found from the particle size distributions of NFC4 and LNFC4 (Fig. 4b). This indicated that lignin-containing fibers contributed to uniform and small size properties of the microfibrillated products during the high-pressure homogenization process, which prevented the aggregation of microfibrillated cellulose. The results were consistent with the particle size distribution conclusion in this study. This phenomenon may be attributed to the lignin causing an increase in the fiber resistance to the mechanical action of the high-pressure homogenization process (Solala *et al.* 2012), and lignin-containing NFC maintaining hydrophobic groups to prevent hydrogen bonding between fibers (Park *et al.* 2017).

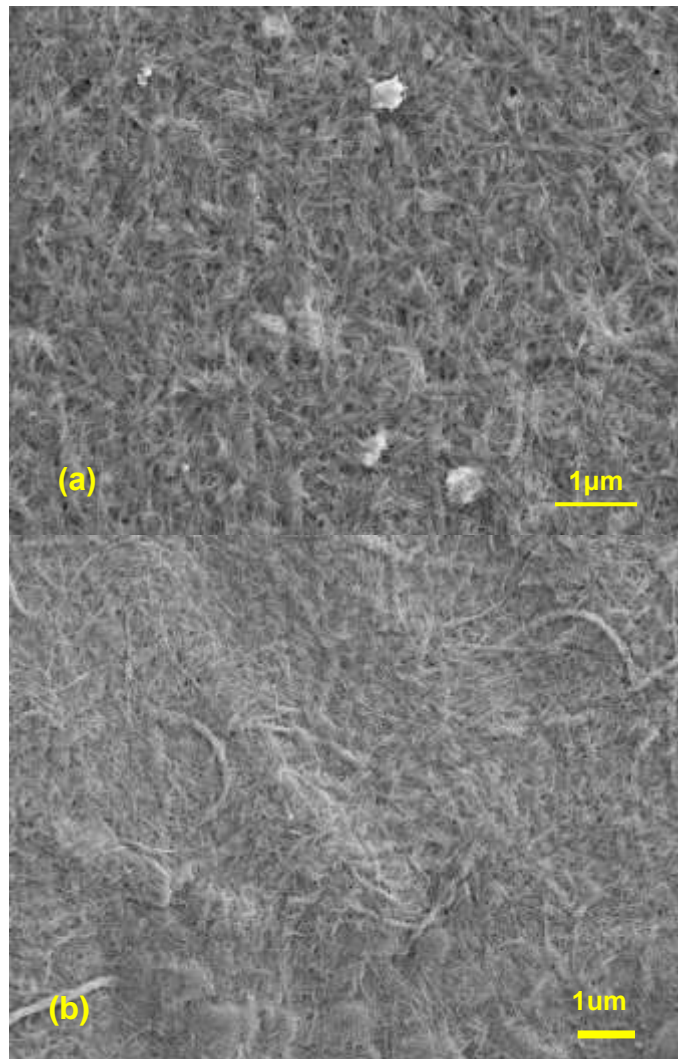


Fig. 3. The SEM morphology of NFC (a) \times 10.0k and LNFC (b) \times 10.0k obtained from twenty cycles of the high-pressure homogeneous process at 25000 psi

Particle Size Analysis

The particle size and its distribution of cellulose microfibrils samples obtained from 2 and 20 high-pressure homogeneous cycles were measured, and the results are shown in Fig. 4 and Table 2. As shown in Fig. 4a, the curves of particle size distributions for NFC1 and LNFC1 almost overlapped, demonstrating that similar particle size distributions can be produced under low homogenization cycles and pressure conditions (Gabiatti *et al.* 2020). As the pressure was increased to 25000 psi, the particle size distribution of NFC2 and LNFC2 were shifted towards a big particle size, and the uniformity values were also increased.

As shown in Table 2, the values of Dv10, Dv50, and Dv90 of NFC2 and LNFC2 samples also reflected that the particle size was increased, and these values of LNFC2 were smaller than that of NFC2. This indicated that the presence of lignin obviously affected the homogeneity of microfibrillated cellulose during high pressure and less homogenization cycles. Lignin can inhibit hydrogen bonding between cellulose fibers, and weak the binding force of microfibrils leading to the crystallinity value decrease, and then reduce the agglomeration of microfibrils to form flocculus aggregates (Shao and Li 2006).

As shown in Fig. 4b, as the homogenization cycles increased to 20, the particle size homogeneity of NFC3 and LNFC3 were reduced for 2500 psi pressure homogenization process, while the particle size homogeneity of NFC4 and LNFC4 were obviously increased for 25000 psi homogenization process, especially for LNFC4 samples. The uniformity value of LNFC4 was smaller than that of NFC4 (Table 2), which indicated that lignin obviously improved the homogeneity of microfibrillated cellulose during high pressure and high homogenization cycles, and the analysis of SEM also obtained similar results. The possible reason for this phenomenon is that the presence of lignin reduces the absorption and swelling of the fibers, improves the strength performance of the fibers, making the micro fibrillation process more difficult (Morales-Medina *et al.* 2020), while lignin-containing NFC also reduces the formation of hydrogen bonds between microfibrils, thereby promoting the homogeneity of micro fibrillated cellulose under high pressure and high homogenization cycles conditions (Hettrich *et al.* 2014).

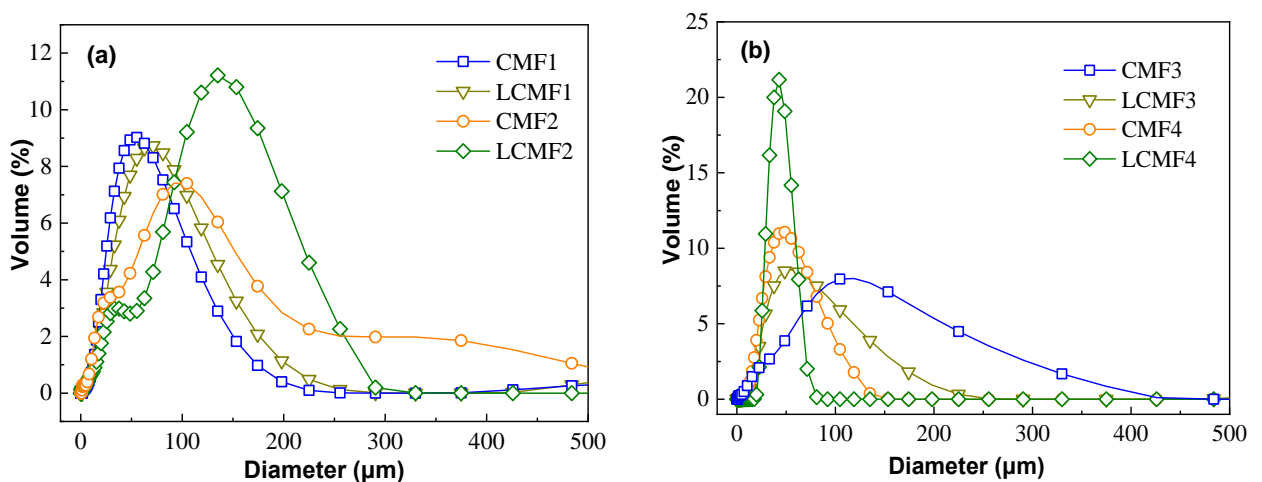


Fig. 4. Particle size distributions of cellulose microfibrils obtained from two and twenty high-pressure homogeneous cycles, (a): two cycles, (b): twenty cycles

As shown in Table 2, the crystallinity values of NFC and LNFC were increased with the homogenization pressure and cycles increasing, and the crystallinity value of

NFC1 was lower than materials and others samples (Table 2 and Fig. S1). The main reason for this phenomenon is that i) The treatment with neutral cellulose and mechanical grinding may reduce the initial crystallinity index (Qing *et al.* 2013; Chen *et al.* 2017), ii) under the low homogenization pressure and homogenization times, cellulose fiber is mainly the splitting and broom of fiber bundles, and the homogenization has little effect on the crystallization area and amorphous area. However, as the homogenization pressure and homogenization times increase, the homogenization will destroy the amorphous regions of fiber more, which will lead to the increase of crystallinity value.

Table 2. The Cellulose Microfibrils Properties

Samples	Uniformity	Dv10/ μm	Dv50/ μm	Dv90/ μm	Crystallinity/%
NFC1	0.47	21 \pm 0.82	75 \pm 1.70	226 \pm 2.45	36.6 \pm 0.33
LNFC1	0.46	21 \pm 1.25	86 \pm 1.25	193 \pm 0.94	42.5 \pm 0.24
NFC2	1.06	23 \pm 0.82	193 \pm 2.05	352 \pm 2.87	41.6 \pm 0.29
LNFC2	0.96	21 \pm 1.25	142 \pm 0.82	243 \pm 1.70	43.5 \pm 0.29
NFC3	0.66	28 \pm 0.82	150 \pm 1.25	288 \pm 2.36	46.2 \pm 0.66
LNFC3	0.52	27 \pm 1.25	81 \pm 0.82	157 \pm 1.70	45.3 \pm 0.34
NFC4	0.43	21 \pm 0.94	44 \pm 0.82	83 \pm 1.63	47.8 \pm 0.21
LNFC4	0.31	14 \pm 0.47	28 \pm 0.94	66 \pm 1.25	46.7 \pm 0.34

Dispersion Stability Analysis

The effect of lignin on the colloidal stability of aqueous NFC suspensions was quantified by a turbiscan lab analyzer, and the homogenization pressure increased from 2500 psi to 25000 psi, the TSI (turbiscan stability index) of aqueous cellulose microfibrils suspensions presented a declining tendency, which indicated an increase in colloidal stability (Figs. 5a and 5b). Specifically, lignin has an important effect on the stability of cellulose microfibrils suspension for two homogenization cycles. The reason for this phenomenon may be that lignin enhanced the microfibrillated cellulose during high pressure with fewer homogenization cycles and decreased the particle size of cellulose microfibrils samples (Fig. 4a).

As shown in Fig. 5b, enhanced stability of the aqueous cellulose microfibrils suspensions was achieved for 2500 psi and twenty homogenization cycles, but their corresponding TSI-time curves were almost overlapping. This indicated that the number of homogenization cycles also had an important effect on the homogeneity of the cellulose microfibrils suspensions. As the homogenization pressure was increased up to 25000 psi, the lignin-containing aqueous cellulose microfibrils suspensions exhibited the lowest TSI values, indicating that the stability increased significantly and in agreement with the particle size results described above (Sun *et al.* 2019). Previous studies also showed that high-pressure homogenization is an effective tool to increase the stability of cellulose systems (Lin *et al.* 2015). Meanwhile, it was shown the particle size of cellulose microfibrils in the presence of lignin was more uniform (Fig. 4b). Due to this fact, the most probable mechanism of the system stabilization was the similar compatibility principle, namely that lignin on the NFC surface limited the combination of hydroxyl group and water, reduced the agglomeration between cellulose microfibrils, and leading to the enhanced stability of the aqueous cellulose microfibrils suspensions. Lignin and hemicellulose bind to cellulose in the cell wall, and thus improve the analysis presented, leading to the greater stability of the aqueous NFC suspensions (Gorshkova *et al.* 2010)

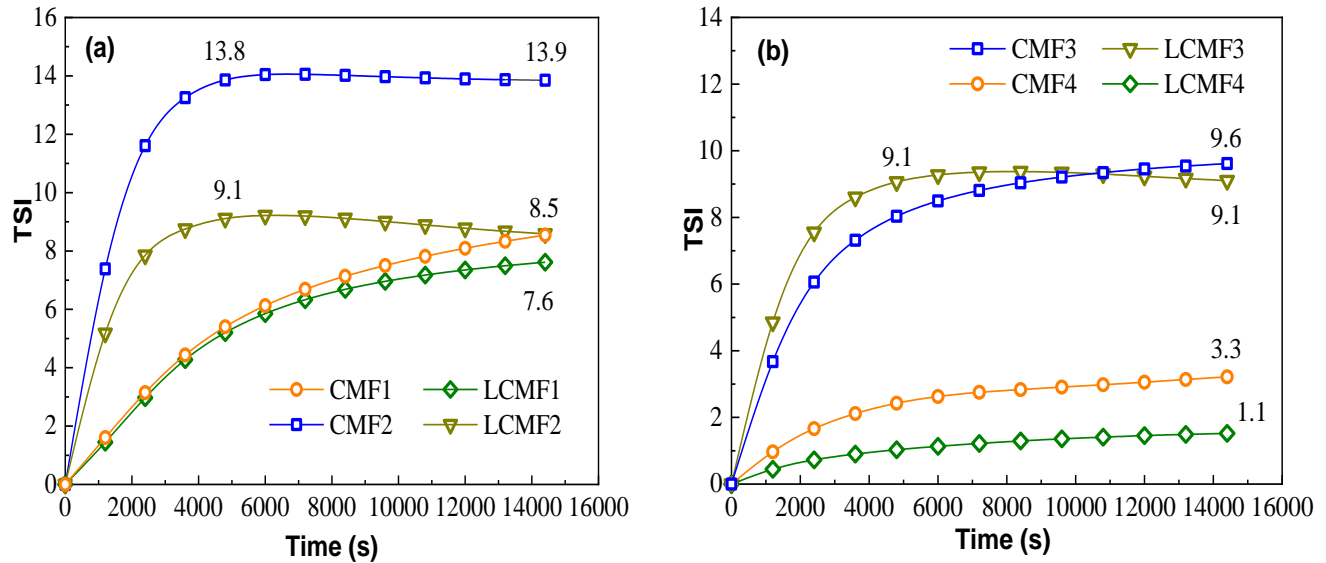


Fig. 5. The suspension stability of cellulose microfibrils obtained from two and twenty high-pressure homogenization cycles, (a): two cycles, (b): twenty cycles

Organic Dye Adsorption Performance Analysis

To study the adsorption behavior of organic dyes with different amounts of NFC and LNFC, three organic dyes suspension samples with 10%, 20%, and 30% NFC4 and LNFC4 addition were prepared. The effects of NFC4 and LNFC4 addition amount on the adsorption performance of organic dye are shown in Fig. 6. From Fig. 6a, as the addition of adsorbent NFC4 with 0, 10%, 20%, and 30%, the TSI values of the four organic dyes suspension samples were 3.53, 1.54, 1.06, and 1.90, respectively. As one can see, pure organic dye suspended into the background aqueous solution was not stable. This indicated that the adsorption stability of organic dye with adding NFC4 as adsorbent was better than that without NFC4. Furthermore, the TSI data also showed that with the increase of NFC4 concentration, the adsorption stability of organic dye increased first and then decreased. The main possible reason was that with the increase of NFC4 concentration, cellulose microfibrils formed a protective layer around organic dye particles, which reduced the repulsive force of aqueous solution on organic dye particles, increased the adsorption stability of organic dye. However, as the dosage of NFC4 exceeds a certain value, the agglomeration of cellulose microfibrils may occur due to the hydrogen bond and the intermolecular force of the layer surface (Mazloumi *et al.* 2018).

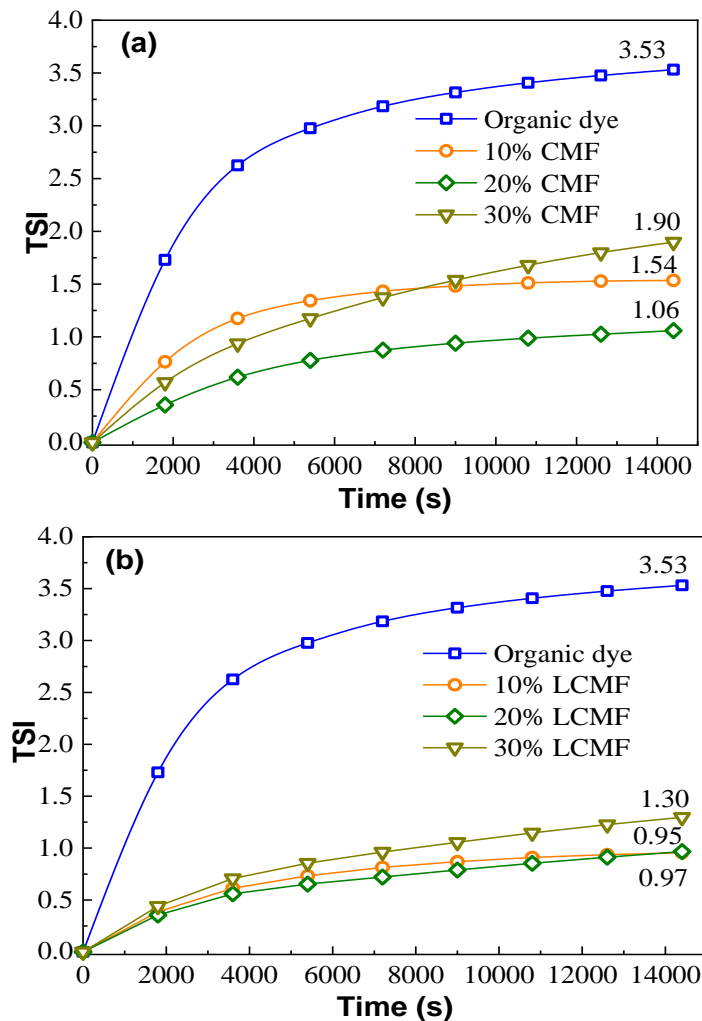


Fig. 6. Effect of addition amount of NFC and LNFC on the dispersion performance of organic dye

As shown in Fig. 6b, as the addition of adsorbent LNFC4 was 10%, 20%, and 30%, the TSI values of the three organic dyes suspension samples were 0.97, 0.95, and 1.30, respectively. The TSI values decreased rapidly as the 10% LNFC4 addition experiment and 20% LNFC4 addition sample reached a stable level, which is the evidence of the organic dye suspension stability, while as the addition amount increases to 30%, the stability of organic dyes suspension decreased. The other observation was that LNFC had a better stabilizing effect on organic dyes suspension than NFC. The possible reason was that lignin reduced surface-chemical polarity of cellulose microfibrils and enhanced cellulose microfibrils compatibility with non-polar media (Tan *et al.* 2016). The hydrophobic groups of the LNFC can adsorb with organic dye particles, leading to the increased hydrophilicity of the organic dye particles, and the dispersion stability of organic dye particles in water was increased. Due to this fact, the most probable mechanism of the system stabilization for NFC and LNFC are different. So, an attempt was made to explain the mechanism of interaction between dye particle, NFC, and LNFC. The suggested mechanisms were presented in Fig. 7.

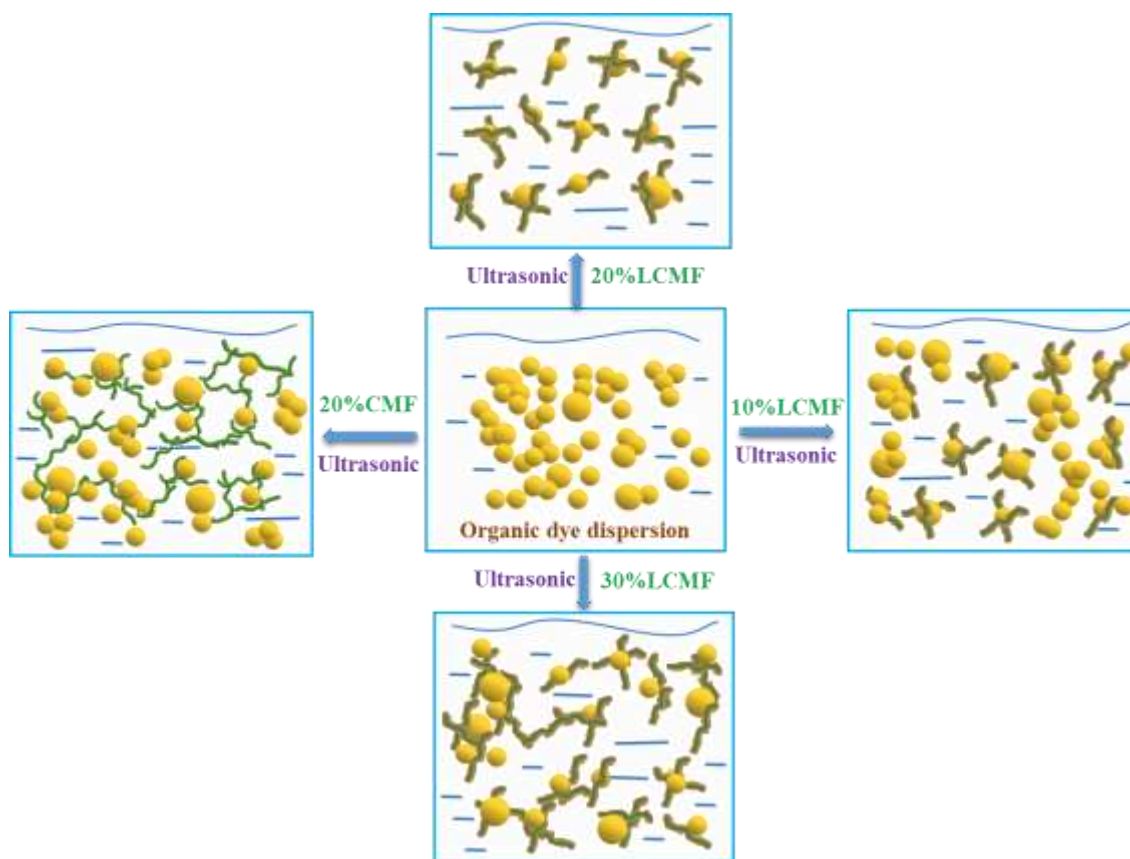


Fig. 7. The effect mechanism of NFC and LNFC on the adsorption performance of organic dye

Figure 7 shows a stability variation simulation diagram of organic dye particle dispersion with the increase of LNFC4 addition amount from 10% to 30%. This implies that the dye-lignin complex is only weakly adsorbed, and adsorption and desorption happen simultaneously. The dye-lignin complex on the surface of cellulose microfibrils is likely to avoid the aggregation of dye particles, upon which they will take on an extended conformation in solution. However, these surface-induced complexes can then re-adsorb and cause flocculation, and the surface-induced complex is affected by the addition amount, which explains why flocculation occurs even at high LNFC4 dosages; desorption results in bare surface, which can subsequently be bridged to another surface by LNFC-LNFC clusters (van der Ven 2005). Therefore, when preparing organic dye suspensions dispersed with lignin-containing cellulose microfibrils, there is a need to choose the appropriate addition amount. There is also a need to determine whether such stabilized dye mixtures are still able to perform well in the dyeing of other materials. The organic orange dye with stable dispersion by LNFC4 will be further adsorbed on textile fibers in the subsequent dyeing process, which guiding significance for the development of new degradable organic dye adsorption dispersants.

CONCLUSIONS

1. The morphological properties and adsorption characteristics of highly fibrillated cellulose (denoted NFC in this article) and lignin-containing cellulose microfibrils (LNFC) were investigated. The morphological properties of cellulose microfibrils were

positively affected by lignin-containing, especially applied in high-pressure fluidization processing.

2. It was more favorable to use lignin-containing fibers in high-pressure fluidization to gain micro- or nanofibrillated cellulose with higher levels of structural fibrillation that reflected both in high uniform particle size and high crystallinity.
3. The mechanical fluidization impact energy could be directed into microfabrication deformations, providing more efficient fibrillation traces for lignin-containing cellulose microfibrils, while softening, bending, splitting filaments, and agglomeration processes were observed from cellulose microfibrils produce process.
4. The role of lignin in adsorbing organic dyes suspension appeared to be mainly based on its hydrophobic character, which reflects the need to choose the appropriate addition amount.

ACKNOWLEDGMENTS

This work was supported by the Zhejiang Provincial Natural Science Foundation of China (Grant LY20C160006), the Key Special Subject of Science and Technology Program of Zhejiang Province (Grant 2020C02043), the open fund of Key Laboratory of Pulp and Paper Science and Technology of Ministry of Education of China, Qilu University of Technology (Grant KF201824), the National Natural Science Foundation of China (Grant 31500492).

REFERENCES CITED

- Aditiawati, P., Dungani, R., and Amelia, C. (2018). "Enzymatic production of cellulose nanofibers from oil palm empty fruit bunch (EFB) with crude cellulase of *Trichoderma* sp.," *Materials Research Express* 5(3), 034005. DOI: 10.1088/2053-1591/aab449
- Baheti, V. and Militky, J. (2013). "Reinforcement of wet milled jute nano/micro particles in polyvinyl alcohol films," *Fibers and Polymers* 14(1), 133-137. DOI: 10.1007/s12221-013-0133-4
- Bian, H., Chen, L., Dai, H., and Zhu, J. Y. (2017a). "Integrated production of lignin containing cellulose nanocrystals (LCNC) and nanofibrils (LCNF) using an easily recyclable di-carboxylic acid," *Carbohydrate Polymers* 167, 167-176. DOI: 10.1016/j.carbpol.2017.03.050
- Bian, H., Chen, L., Gleisner, R., Dai, H., and Zhu, J. Y. (2017b). "Producing wood-based nanomaterials by rapid fractionation of wood at 80 °C using a recyclable acid hydrotrope," *Green Chemistry* 19(14), 3370-3379. DOI: 10.1039/c7gc00669a
- Bian, H., Dong, M., Chen, L., Zhou, X., Ni, S., Fang, G., and Dai, H. (2019). "Comparison of mixed enzymatic pretreatment and post-treatment for enhancing the cellulose nanofibrillation efficiency," *Bioresource Technology* 293, 122171. DOI: 10.1016/j.biortech.2019.122171
- Bian, H., Dong, M., Chen, L., Zhou, X., Wang, R., Jiao, L., Ji, X., and Dai, H. (2020). "On-demand regulation of lignocellulosic nanofibrils based on rapid fractionation using acid hydrotrope: kinetic study and characterization. *ACS Sustainable Chemistry & Engineering* 8(25), 9569-9577. DOI: 10.1021/acssuschemeng.0c02968

- Cai, C., Hirth, K., Gleisner, R., Lou, H., Qiu, X., and Zhu, J. Y. (2020). "Maleic acid as a dicarboxylic acid hydrotrope for sustainable fractionation of wood at atmospheric pressure and ≤ 100 °C: mode and utility of lignin esterification," *Green Chemistry* 22(5), 1605-1617. DOI: 10.1039/c9gc04267a
- Chen, Y., Fan, D., Han, Y., Li, G., and Wang, S. (2017). "Length-controlled cellulose nanofibrils produced using enzyme pretreatment and grinding," *Cellulose* 24(12), 5431-5442. DOI: 10.1007/s10570-017-1499-z
- Chinga-Carrasco, G., Kuznetsova, N., Garaeva, M., Leirset, I., Galiullina, G., Kostochko, A., and Syverud, K. (2012). "Bleached and unbleached NFC nanobarriers: Properties and hydrophobisation with hexamethyldisilazane," *Journal of Nanoparticle Research* 14(12), 1280. DOI: 10.1007/s11051-012-1280-z
- Ehman, N. V., Lourenço, A. F., McDonagh, B. H., Vallejos, M. E., Felissia, F. E., Ferreira, P. J. T., Chinga-Carrasco, G., and Area, M. C. (2020). "Influence of initial chemical composition and characteristics of pulps on the production and properties of lignocellulosic nanofibers," *International Journal of Biological Macromolecules* 143, 453-461. DOI: 10.1016/j.ijbiomac.2019.10.165
- Gabiatti, C., Jr., Neves, I. C. O., Lim, L. T., Bohrer, B. M., Rodrigues, R. C., and Prentice, C. (2020). "Characterization of dietary fiber from residual cellulose sausage casings using a combination of enzymatic treatment and high-speed homogenization," *Food Hydrocolloids* 100, 105398. DOI: 10.1016/j.foodhyd.2019.105398
- Gorshkova, T. A., Mikshina, P. V., Gurjanov, O. P., and Chemikosova, S. B. (2010). "Formation of plant cell wall supramolecular structure," *Biochemistry (Mosc)* 75(2), 159-172. DOI: 10.1134/S0006297910020069
- Gourlay, K., van der Zwan, T., Shourav, M., and Saddler, J. (2018). "The potential of endoglucanases to rapidly and specifically enhance the rheological properties of micro/nanofibrillated cellulose," *Cellulose* 25(2), 977-986. DOI: 10.1007/s10570-017-1637-7
- Herzele, S., Veigel, S., Liebner, F., Zimmermann, T., and Gindl-Altmutter, W. (2016). "Reinforcement of polycaprolactone with microfibrillated lignocellulose," *Industrial Crops and Products* 93, 302-308. DOI: 10.1016/j.indcrop.2015.12.051
- Hettrich, K., Pinnow, M., Volkert, B., Passauer, L., and Fischer, S. (2014). "Novel aspects of nanocellulose," *Cellulose* 21(4), 2479-2488. DOI: 10.1007/s10570-014-0265-8
- Kawee, N., Lam, N. T., and Sukyai, P. (2018). "Homogenous isolation of individualized bacterial nanofibrillated cellulose by high pressure homogenization," *Carbohydrate Polymers* 179, 394-401. DOI: 10.1016/j.carbpol.2017.09.101
- Lê, H. Q., Dimic-Misic, K., Johansson, L.-S., Maloney, T., and Sixta, H. (2018). "Effect of lignin on the morphology and rheological properties of nanofibrillated cellulose produced from γ -valerolactone/water fractionation process," *Cellulose* 25(1), 179-194. DOI: 10.1007/s10570-017-1602-5
- Lin, D., Li, R., Lopez-Sanchez, P., and Li, Z. (2015). "Physical properties of bacterial cellulose aqueous suspensions treated by high pressure homogenizer," *Food Hydrocolloids* 44, 435-442. DOI: 10.1016/j.foodhyd.2014.10.019
- Lissi, E. A. and Abuin, E. B. (2000). "A general treatment for meaningful comparison of rate parameters of enzyme-catalyzed reactions in aqueous and reverse micellar solutions," *Langmuir* 16(26), 10084-10086. DOI: 10.1021/la000788z
- Mazloumi, M., Johnston, L. J., and Jakubek, Z. J. (2018). "Dispersion, stability and size measurements for cellulose nanocrystals by static multiple light scattering," *Cellulose* 25(10), 5751-5768. DOI: 10.1007/s10570-018-1961-6

- Morales-Medina, R., Dong, D., Schalow, S., and Drusch, S. (2020). "Impact of microfluidization on the microstructure and functional properties of pea hull fibre," *Food Hydrocolloids* 103, 105660. DOI: 10.1016/j.foodhyd.2020.105660
- Park, C.-W., Han, S.-Y., Namgung, H.-W., Seo, P.-n., Lee, S.-Y., and Lee, S.-H. (2017). "Preparation and characterization of cellulose nanofibrils with varying chemical compositions," *BioResources* 12(3), 5031-5044. DOI: 10.15376/biores.12.3.5031-5044
- Qing, Y., Sabo, R., Zhu, J. Y., Agarwal, U., Cai, Z., and Wu, Y. (2013). "A comparative study of cellulose nanofibrils disintegrated via multiple processing approaches," *Carbohydrate Polymers* 97(1), 226-234. DOI: 10.1016/j.carbpol.2013.04.086
- Ren, S., Sun, X., Lei, T., and Wu, Q. (2014). "The effect of chemical and high-pressure homogenization treatment conditions on the morphology of cellulose nanoparticles," *Journal of Nanomaterials* 2014, 582913. DOI: 10.1155/2014/582913
- Rivers, G., Yu, L., and Zhao, B. (2019). "Cellulose nanocrystal and silver nanobelt gel: cooperative interactions enabling dispersion, colloidal gels, and flexible electronics," *Langmuir* 35(48), 15897-15903. DOI:10.1021/acs.langmuir.9b02003
- Santucci, B. S., Bras, J., Belgacem, M. N., da Silva Curvelo, A. A., Borges Pimenta, M. T. (2016). "Evaluation of the effects of chemical composition and refining treatments on the properties of nanofibrillated cellulose films from sugarcane bagasse," *Industrial Crops and Products* 91, 238-248. DOI: 10.1016/j.indcrop.2016.07.017
- Shao, Z. and Li, K. (2006). "The effect of fiber surface lignin on interfiber bonding," *Journal of Wood Chemistry & Technology* 26(3), 231-244. DOI: 10.1080/02773810601023438
- Solala, I., Volperts, A., Andersone, A., Dizhbite, T., Mironova-Ulmane, N., Vehniäinen, A., Pere, J., and Vuorinen, T. (2012). "Mechanoradical formation and its effects on birch kraft pulp during the preparation of nanofibrillated cellulose with Masuko refining," *Holzforschung* 66(4), 477-483. DOI: 10.1515/hf.2011.183
- Sun, C., Fang, Z., Qin, F., Chen, K., Wang, J., Ding, Z., and Qiu, X. (2019). "Insight into the dispersive mechanism of carboxylated nanofibrillated cellulose for individual montmorillonite in water," *Composites Part B: Engineering* 177, article no. 107399. DOI: 10.1016/j.compositesb.2019.107399
- Taheri, H. and Samyn, P. (2016). "Effect of homogenization (microfluidization) process parameters in mechanical production of micro- and nanofibrillated cellulose on its rheological and morphological properties," *Cellulose* 23(2), 1221-1238. DOI: 10.1007/s10570-016-0866-5
- Tan, Y., Liu, Y., Chen, W., Liu, Y., Wang, Q., Li, J., and Yu, H. (2016). "Homogeneous dispersion of cellulose nanofibers in waterborne acrylic coatings with improved properties and unreduced transparency," *ACS Sustainable Chemistry & Engineering* 4(7), 3766-3772. DOI: 10.1021/acssuschemeng.6b00415
- Vanhatalo, K., Lundin, T., Koskimäki, A., Lillandt, M., and Dahl, O. (2016). "Microcrystalline cellulose property-structure effects in high-pressure fluidization: microfibril characteristics," *Journal of Materials Science* 51(12), 6019-6034. DOI: 10.1007/s10853-016-9907-6
- Velasquez-Cock, J., Gañán, P., Posada, P., Castro, C., Serpa, A., Gómez H. C., Putaux, J. -L., and Zuluaga, R. (2016). "Influence of combined mechanical treatments on the morphology and structure of cellulose nanofibrils: Thermal and mechanical properties of the resulting films," *Industrial Crops and Products* 85, 1-10. DOI: 10.1016/j.indcrop.2016.02.036
- van der Ven, T. G. M. (2005). "Association-induced polymer bridging by poly(ethylene

oxide)-cofactor flocculation systems," *Advances in Colloid and Interface Science* 114-115, 147-157. DOI: 10.1016/j.cis.2004.08.002

Wang, Q. Q., Zhu, J. Y., Gleisner, R., Kuster, T. A., Baxa, U., and McNeil, S. E. (2012). "Morphological development of cellulose fibrils of a bleached eucalyptus pulp by mechanical fibrillation," *Cellulose* 19(5), 1631-1643. DOI: 10.1007/s10570-012-9745-x

Wang, W., Liang, T., Bai, H., Dong, W., and Liu, X. (2018). "All cellulose composites based on cellulose diacetate and nanofibrillated cellulose prepared by alkali treatment," *Carbohydrate Polymers* 179, 297-304. DOI: 10.1016/j.carbpol.2017.09.098

Article submitted: May 5, 2021; Peer review completed: June 20, 2021; Revised version received and accepted: July 25, 2021; Published: August 4, 2021.
DOI: 10.15376/biores.16.4.6560-6576

APPENDIX

Supplementary Material

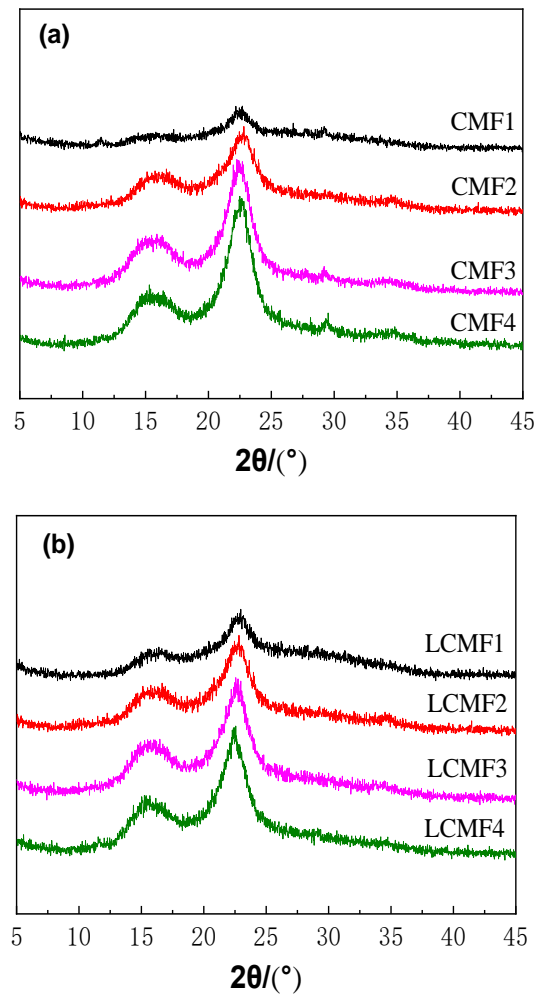


Fig. S1. The X-ray diffractograms of cellulose microfibrils obtained from two and 20 high-pressure homogeneous cycles, (a): NFC, (b): LNFC